Synthetic Metals 232 (2017) 96–102

Contents lists available at ScienceDirect

Synthetic Metals

journal homepage: www.elsevier.com/locate/synmet

Acceptor and donor substituted alkoxy(phenyleneethynylenes) (Alkoxy-PEs): Synthesis, thermal, linear and nonlinear optical properties

Md. Khairul Amin[a,1], Md. Mostafizur Rahman[a,1], Masnun Naher[a,1], Tanjila Islam[a,1], Md. Faruak Ahmad[a], Md. Amran-al-taz Khan[a], Mohammad Mizanur Rahman Khan[a], Md. Ashraful Alam[a], Muhammad Younus[a,*], Manash Kanti Biswas[b,1], Yasmeen Haque[b]

[a] Department of Chemistry, Shahjalal University of Science and Technology, Sylhet 3114, Bangladesh
[b] Department of Physics, Shahjalal University of Science and Technology, Sylhet 3114, Bangladesh

ARTICLE INFO

Keywords:
Alkoxy(phenyleneethynylenes)
Thermal stability and third-order nonlinearity

ABSTRACT

A series of acceptor and donor substituted bis(alkoxy)phenyl ethynyl oligomers 4,4′-((2,5-alkyoxy-1,4-phenylene)bis(ethyne-2,1-diyl))bis(nitrobenzene) (alkyl = C_4H_9 **3a;** C_8H_{17} **3b** and $C_{12}H_{25}$ **3c**) and 4,4′-((2,5-alkyoxy-1,4-phenylene)bis(ethyne-2,1-diyl))bis(methylbenzene) (alkyl = C_4H_9 **4a;** C_8H_{17} **4b** and $C_{12}H_{25}$ **4c**) has been synthesized by the palladium catalyzed cross coupling reaction of 1,4-dialkoxy-2,5-diiodobenzene with appropriate alkynes. The newly synthesized products were characterized by UV–Vis, IR and multinuclear NMR spectroscopic techniques as well as elemental analyses. All the synthesized bis-(alkoxy)phenyl ethynyl derivatives exhibit good thermal stability (T_5 = 329–347 °C) as evident by thermo gravimetric analysis. In nitrophenyl substituted **3a-c**, emission is observed in the green region, while in tolyl substituted **4a-c**, emission is observed in the blue region of the electromagnetic radiation. Continuous wave (CW) closed aperture Z-scan technique reveals the signature of third-order nonlinearity in the materials that are thermal in nature.

1. Introduction

For the last two decades, there have been tremendous efforts in the development of conjugated small molecules, oligomers and polymers for their applications in field-effect transistors, photodectors, photovoltaics and electroluminescence devices [1–5]. These materials are composed of unsaturated units that have extended π-orbitals, thus enabling optical absorption and proper charge transport [6–8]. The extent of conjugation/interaction between these units determines the solution/solid state electronic structure, which in turn controls key material properties such as optical absorption/emission, frontier molecular orbital energy levels (HOMO and LUMO) and redox characteristics [1a]. The π-conjugated system can possess an extremely high optical nonlinear response due to the fact that the π electrons in this kind of material tend to be delocalized more easily and the value of linear and third-order nonlinear polarizabilities can be related to the number of electrons per unit length [9].

Among the conjugated polymers, poly(*p*-phenyleneethynylenes) (PPEs) are promising for their ease of preparation, solution processability and wide range of materials properties [10]. Palladium is an efficient catalyst for the coupling reaction of bis-(alkynyl)arenes with dihaloarenes to synthesize PPEs [10–12]. However, initial efforts to form PPEs resulted in low-molecular-weight oligomers with poor solubility [13–15]. To overcome these problems, researchers had utilized long-chain alkyl or alkoxy substituted arenes as monomers which gave high molecular weight rigid-rod polymers with good solubility [10a,16]. Though, PPEs are strong candidates for the fabrication of optoelectronic devices [10b,17], they usually do not have well-defined structures, and are often polydisperse, which affect the optical properties [17b]. As an alternative, π-conjugated small molecules and oligomers are attractive due to their exact molecular weight, high purities and defect-free structures [18]. To cite examples of this class of materials, arylene ethynylenes [19] (e.g. phenylene, fluorene, pyrene, carbazole) with high fluorescence quantum yield have been studied for OLED device fabrication [19b–c]. The device fabrication and operational lifetime of these materials depend on their good thermal and morphological stability [20].

Oligo- and poly-phenyleneethynylenes, oligo-phenylenevinylene and hybrid poly-phenyleneethylylene/phenylenevinylene have been extensively studied for third-order nonlinear optics (NLO) [21a–d]. These types of conjugated organic oligomers and polymers and other organic conjugated dyes [21e–f] gained importance as NLO materials

* Corresponding author.
E-mail address: myounus-che@sust.edu (M. Younus).
[1] Authors have equal contributions.

http://dx.doi.org/10.1016/j.synthmet.2017.06.005
Received 19 December 2016; Received in revised form 29 May 2017; Accepted 6 June 2017

because of low cost, ease in processing, enhanced properties and biodegradable qualities. The materials exhibiting high optical nonlinearities have potential of being a suitable candidate for high density optical data storage, photodynamic therapy and optical limiters [9,29a].

In this study, we report the synthesis and characterization of a new series of substituted bis-(alkoxy)phenyleneethynylenes and investigations of their thermal, linear (absorption and photoluminescence) and nonlinear (third-order) optical properties.

2. Experimental details

2.1. Materials and techniques

All the reactions were performed under nitrogen atmosphere with special Schlenk techniques [22]. Solvents were dried, and freshly distilled from appropriate drying agents [22]. All chemical reagents were purchased from commercial suppliers and used without further purification. The compounds $H_9C_4O{-}C_6H_2I_2{-}OC_4H_9$ [23], $H_{17}C_8O{-}C_6H_2I_2{-}OC_8H_{17}$ [23], and $H_{25}C_{12}O{-}C_6H_2I_2{-}OC_{12}H_{25}$ [23], and $HC{\equiv}C{-}C_6H_4{-}CH_3$ [24] and $HC{\equiv}C{-}C_6H_4{-}NO_2$ [24] were prepared following literature methods. NMR spectra were measured with Bruker 400FT NMR spectrometer in $CDCl_3$ solvent. ^1H NMR spectra were referenced to 7.25 ppm (residual proton of $CHCl_3$) of $CDCl_3$, and ^{13}C NMR spectra were referenced to solvents resonances. Infrared spectra were undertaken on a Shimadzu FTIR prestige 21 spectrometer as KBr pellets or dichloromethane solution. Microanalyses were carried out at Bangladesh Council for Scientific Research Laboratory (BCSIR), Dhaka, Bangladesh. Thermal analysis (Thermo gravimetry analysis, TGA) was obtained by using TGA-50 thermogravimetric analyzer under flowing nitrogen. Samples were heated, at 10 °C/min, in aluminium crucibles. The phase transition temperatures and associated enthalpies during phase transition were obtained using differential scanning calorimetry (DSC) in Shimadzu TA-60A instrument. Heating and cooling rates were set at 10 °C/min under nitrogen atmosphere. The UV–Vis spectra were measured using Shimadzu UV-1800 spectrometer. The photoluminescence (PL) spectra were measured with Shimadzu RF–3501 pc spectrofluorometer. A continuous wave (cw) Ar-ion laser at 514 nm on power 19.35 mW was used to determine the nonlinear refractive index (n_2) of **3a-c** and **4a-c**. Toluene was used as solvent, and measurements were done in six different concentrations ranging from 1e-4 to 1e-3 mol/L. A convex lens of 7.56 cm focal length was used to focus the Gaussian laser beam. The liquid sample is contained in a quartz cuvette of width 2 mm. The focusing lens has a focal length of 7.56 cm. Translation of the sample along z-axis has been ensured by a motorized translational stage (Fig. 1). Baseline correction was made by using toluene as background. Three sets of reading were taken for each sample and standard deviation, from the calculated values, were used as experimental error.

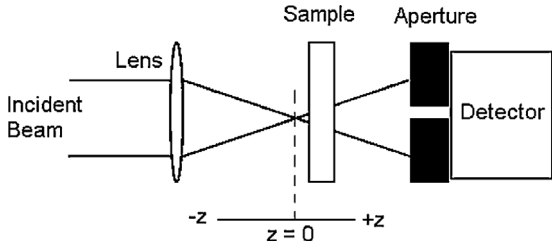

Fig. 1. Schematic diagram of closed aperture Z-scan technique.

2.2. Syntheses of substituted bis(alkoxy)ethynylarylethynyl derivatives (3 and 4)

2.2.1. 4,4′-((2,5-dibutoxy-1,4-phenylene)bis(ethyne-2,1-diyl))bis (nitrobenzene) (3a)

To a mixture of 1,4-dibutoxy-2,5-diiodobenzene (**1a**) (0.1 g, 0.21 mmol) and *p*-nitrophenylacetylene (**2a**) (0.077 g, 0.53 mmol) in presence of $Pd[PPh_3]_2Cl_2$ (0.003 g, 2% mmol), CuI (0.0008 g, 2% mmol) and PPh_3 (0.002 g, 4% mmol) in diisopropylamine (20 mL) was degassed with nitrogen atmosphere, and the resulting mixture was stirred for 18 h at 65 °C. After completion of the reaction, diethylether was added to the reaction mixture, and the precipitate was removed by filtration. The solvent was removed under vacuum, and the solid residue was redissolved in diethylether, and the resulting solution was washed with 10% HCl acid followed by brine solution, and dried over anhydrous magnesium sulfate. After that, the solvent was removed under reduced pressure, and the solid residue was purified on silica column chromatography, using hexane and dichloromethane (2:1), to obtain **3a** as a bright yellow solid in 55% (0.059 g) yield. IR (solid state, KBr): ν 3047, 2962 (C–H str.), 2205 (C≡C str.), 1217 (C–O str.) cm^{-1}; ^1H NMR (400 MHz, $CDCl_3$): δ 1.01 (t, 6H, CH_3), 1.57 (s, 4H, CH_2), 1.84 (q, 4H, CH_2), 4.05 (t, ^3J = 6.4 Hz, 4H, OCH_2), 7.03 {s, 2H, $(RO)_2$Ar-H}, 7.65 (d, ^3J = 8.80 Hz, 4H, Ar-H), 8.25 (d, ^3J = 8.80 Hz, 4H, Ar-H); ^{13}C NMR (100 MHz, $CDCl_3$): δ 13.90, 19.29, 31.31, 69.34, 91.21, 93.38, 113.86, 116.83, 123.72, 130.29, 132.21, 147.06, 153.97; Anal. Calc. for $C_{30}H_{28}N_2O_6$: C, 70.30; H, 5.51; N, 5.47%. Found: C, 69.83; H, 5.52; N, 5.33%.

2.2.2. 4,4′-((2,5-dioctayloxy-1,4-phenylene)bis(ethyne-2,1-diyl))bis (nitrobenzene) (3b)

The compound **3b** was synthesized using similar procedure as described above for **3a** by using 1,4-dioctyloxy-2,5-diiodobenzene (**1b**) instead of 1,4-dibutoxy-2,5-diiodobenzene (**1a**). The compound **3b** obtained as a yellow solid in yield 60% (0.064 g). IR (solid state, KBr): ν 3078, 2922 (C–H str.), 2205(C≡C str.), 1224 (C–O str.) cm^{-1}; ^1H NMR (400 MHz, $CDCl_3$): δ 0.85 (bt, 6H, CH_3), 1.24-1.39 (m, 20H, CH_2), 1.85 (q, 4H, CH_2), 4.04 (t, ^3J = 6.0 Hz, 4H, OCH_2), 7.02 {s, 2H, $(RO)_2$Ar-H}, 7.65 (d, ^3J = 8.00 Hz, 4H, Ar-H), 8.22 (d, ^3J = 7.60 Hz, 4H, Ar-H); ^{13}C NMR (100 MHz, $CDCl_3$): δ 14.10, 22.69, 26.10, 28.95, 29.29, 29.35, 31.82, 69.62, 91.22, 93.38, 113.84, 116.80, 123.70, 130.28, 132.22, 147.05, 153.96; Anal. Calc. for $C_{38}H_{44}N_2O_6$: C, 73.05; H, 7.10; N, 4.48%. Found: C, 72.63; H, 7.28; N, 3.99%.

2.2.3. 4,4′-((2,5-didodecyloxy-1,4-phenylene)bis(ethyne-2,1-diyl))bis (nitrobenzene) (3c)

The compound **3c** was synthesized utilizing similar procedure as described above for **3a,** using 1,4-didodecyloxy-2,5-diiodobenzene (**1c**) instead of 1,4-dibutoxy-2,5-diiodobenzene (**1a**). The compound **3c** was obtained as a yellow solid in 90% yield (0.095 g). Spectroscopic data are in accord with the reported **3c** [25a].

2.2.4. 4,4′-((2,5-dibutoxy-1,4-phenylene)bis(ethyne-2,1-diyl))bis (methylbenzene) (4a)

A mixture of 1,4-dibutoxy-2,5-diiodobenzene (**1a**) (0.1 g, 0.21 mmol) and *p*-tolylacetylene (**2b**) (0.06 g, 0.53 mmol) in presence of $Pd[PPh_3]_2Cl_2$ (0.015 g, 10% mmol), CuI (0.004 g, 10% mmol) and PPh_3 (0.011 g, 20% mmol) in diisopropylamine (20 mL) was added to a small double-neck flask and degassed with nitrogen atmosphere, and, then, the resulting mixture was stirred for 18 h at 82 °C. The completion of the reaction was determined by TLC and IR. After completion of the reaction, diethylether was added to the reaction mixture, and the precipitate was removed by filtration. The solvent was removed under vacuum, and the solid residue was redissolved in diethylether. Then, the resulting solution was washed with 10% HCl acid followed by brine solution, and dried over anhydrous magnesium sulfate. After that, the solvent was removed under reduced pressure, and the solid residue was

purified by column chromatography on silica gel eluting with hexane and dichloromethane (3:1). The title compound **4a** was obtained as a pale yellow solid in 52% (0.049 g) yield. Spectroscopic data are in accord with the reported **4a** [25b].

2.2.5. 4,4′-((2,5-dioctayloxy-1,4-phenylene)bis(ethyne-2,1-diyl))bis (methylbenzene) (4b)

The same procedure as for compound **4a** was followed for the synthesis of **4b** by using 1,4-dioctyloxy-2,5-diiodobenzene (**1b**) instead of 1,4-dibutoxy-2,5-diiodobenzene (**1a**). The compound **4b** obtained as a pale yellow solid in yield 55% (0.053 g). IR (solid state, KBr): ν 3028, 2922 (C−H str.), 2206 (C≡C str.), 1216 (C−O str.) cm^{-1}; ^1H NMR (400 MHz, $CDCl_3$): δ 0.85 (b, 6H, CH_3), 1.26-1.35 (m, 16H, CH_2), 1.50-1.56 (m, 4H, CH_2), 1.82 (q, 4H, CH_2), 2.35 (s, 6H, Ar-CH_3), 4.01 (t, ^3J = 6.4 Hz, 4H, OCH_2), 6.98 {s, 2H, $(RO)_2$Ar-H}, 7.14 (d, ^3J = 7.60 Hz, 4H, Ar-H), 7.42 (d, ^3J = 7.60 Hz, 4H, Ar-H); ^{13}C NMR (100 MHz, $CDCl_3$): δ 14.10, 21.54, 22.69, 26.11, 29.33, 29.42, 31.84, 69.72, 85.35, 95.00, 114.07, 117.04, 120.46, 129.09, 131.49, 138.38, 153.63; Anal. Calc. for $C_{40}H_{50}O_2$: C, 85.36%; H, 8.95%. Found: C, 84.34%; H, 9.08%.

2.2.6. 4,4′-((2,5-didodecyloxy-1,4-phenylene)bis(ethyne-2,1-diyl))bis (methylbenzene) (4c)

The same procedure as for **4a** was utilized for the synthesis of **4c** by using 1,4-didodecyloxy-2,5-diiodobenzene (**1c**) instead of 1,4-dibutoxy-2,5-diiodobenzene (**1a**). The compound **4c** was obtained as a pale yellow solid in 67% yield (0.065 g). IR (solid state, KBr): ν 3035, 2922 (C−H str.), 2212 (C≡C str.), 1216 (C−O str.) cm^{-1}; ^1H NMR (400 MHz, $CDCl_3$): δ 0.87 (t, 6H, CH_3), 1.24-1.36 (m, 32H, CH_2), 1.52 (m, 4H, CH_2), 1.83 (m, 4H, CH_2), 2.36 (s, 6H, Ar-CH_3), 4.01 (t, ^3J = 6.0 Hz, 4H, OCH_2), 6.99 {s, 2H, $(RO)_2$Ar-H}, 7.15 (d, ^3J = 7.60 Hz, 4H, Ar-H), 7.42 (d, ^3J = 7.20 Hz, 4H, Ar-H); ^{13}C NMR (100 MHz, $CDCl_3$): δ 14.13, 21.54, 22.71, 26.11, 29.39, 29.48, 29.66, 29.68, 29.72, 31.95, 69.71, 85.37, 95.0, 114.08, 117.03, 120.47, 129.09, 131.49, 138.36, and 153.63; Anal. Calc. for $C_{48}H_{66}O_2$: C, 85.40%; H, 9.85%. Found: C, 85.62%; H, 10.07%.

3. Results and discussion

3.1. Syntheses

When 1,4-dibutoxy-2,5-diiodobenzene **1a** was treated with *p*-nitrophenylacetylene **2a** in presence of bis(triphenylphosphine)dichloropalladium(II) and copper iodide catalysts in diisopropylamine at 65 °C for 18 h under nitrogen atmosphere, cross coupling reaction [12] (Scheme 1) proceeded to form 4,4′-((2,5-dibutoxy-1,4-phenylene)bis (ethyne-2,1-diyl))bis(*p*-nitrophenylbenzene) **3a** in good yield (55% yield, entry 1, Table 1). The newly synthesized compound **3a** was purified and isolated by column chromatography eluting with hexane and dichloromethane (3:1). Similarly, coupling products with various alkoxy groups and acceptor and donor end groups were also prepared (Scheme 1). The results are summarized in Table 1. Compounds **3b** and **3c** were isolated as bright yellow solids in 60 and 90% yield, respectively (Table 1, entry 2 and 3), and compounds **4a**, **4b**, and **4c** were isolated as pale yellow solids in 52, 55, and 67% yield, respectively (Table 1, entry 4, 5 and 6). Recently, an oxygen free two-chamber reaction system has been developed, which gives 1,4- and 1,3-octyloxy phenyl ethynyl derivatives (benzene, nitrobenzene **3c**, naphthalene, ferrocene etc) and 1,3-azulene ethynyl derivatives (benzene and napthalene) in high yield [25a] (Pd cat. 0.4 mol%, RT, 9 days). On the other hand, we used conventional Sonogashira coupling reaction to form **3c** in 90% (Table 1, entry 3) using mild reaction conditions (2 mol % Pd cat., at 65 °C, 18 h). Compound **4a** has also been reported previously [25b] in three steps reactions starting from diiodobutoxybenzene to bis-trimethysilylacetylene derivative, then to bis-terminal acetylene derivative, and finally to product **4a**. However, we used straight forward Sonogashira coupling reaction of 1,4-dibutoxyphenyl-2,5-diiodide with commercially available tolyl acetylene to form the product **4a**, though the yield of the reaction is low with low catalyst loading. The synthesized coupling products **3a-c** and **4a-c** display in good solubility in common organic solvents, but are insoluble in hexane. So, these compounds are solution processable, which is an essential criterion for low cost device fabrication.

3.2. Characterization

All the products provided satisfactory elemental analysis. The chemical structures of the products **3a-b** and **4b-c** have been confirmed by IR and ^1H and ^{13}C NMR spectroscopic analyses (Table 2). The stretching vibration of ν(C≡C), in the IR spectrum, is diagnostic to the characterization of the ethynyl compounds. The absence of acetylenic hydrogen, ν(≡C−H) vibration gives evidence of the desired cross-coupling reaction (RC≡CR). For example, **3a** displays a single absorption band at 2205 cm^{-1}, confirming the stretching vibration of the ethynyl group (C≡C), but it did not exhibit absorption band in the range of 3200–3300 cm^{-1}, which suggests that the terminal acetylenic group (≡CH) of *p*-nitrophenylacetylene (**2a**) undergoes the coupling with 1,4-dibutoxy-2,5-diiodobenzene (**1a**). Similarly, compound **3b**, **3c**, and **4a**, **4b** and **4c** display characteristic IR peaks in the expected regions (Table 2).

The ^1H NMR spectrum of **3a** displays doublets at 7.65 and 8.22 ppm with coupling constant ^3J = 8.8 Hz which confirms the presence of *para*-substituted benzene ring in the molecule (Fig. 2). A sharp singlet at 7.03 ppm is assigned to the butoxy substituted phenyl ring, and the triplet at 4.05 ppm (^3J = 6.4 Hz) is assigned to the OCH_2 proton of the butoxy chain. The positions of all other NMR signals and their integration ratio are fully consistent with the structure of the molecule (Fig. 2). Similarly, the alkyl, alkoxy and phenyl protons of compound **3b** and **4b, 4c** display ^1H NMR peaks in the desired region of spectra (Table 2).

In the ^{13}C NMR spectra, compound **3a** displays a strong characteristic peak at 69.34 ppm for −OCH_2 carbon, and peaks at 91.21 and 93.38 ppm for acetylenic carbons. The alkyl and phenyl carbons display signals in the desired positions. Similarly, compounds **3b**, **4b**, and **4c**

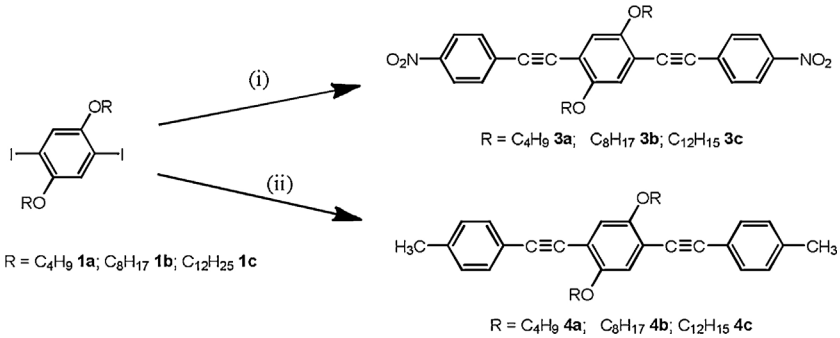

Scheme 1. Synthetic scheme for coupling products **3** and **4**: (i) HC≡C−C_6H_4-4-NO_2 **2a**, $Pd(PPh_3)_2Cl_2$, PPh_3, CuI, $^{iso}Pr_2NH$, (ii) HC≡C−C_6H_4-4-CH_3 **2b**, $Pd(PPh_3)_2Cl_2$, PPh_3, CuI, $^{iso}Pr_2NH$.

Table 1
Synthesis of Alkoxy-PEs by palladium/copper catalyzed coupling reactions[a].

Entry	1,4-dialkoxy-2,5-diiodobenzene, **1** (0.21 mmol)	Arylacetylene, **2** (0.53 mmol)	$Pd[PPh_3]_2Cl_2$ (% mmol)	CuI (% mmol)	Product	Isolated Yield (%)
1	**1a**	**2a**	2	2	**3a**[b]	55
2	**1b**	**2a**	2	2	**3b**[b]	60
3	**1c**	**2a**	2	2	**3c**[b]	90
4	**1a**	**2b**	10	10	**4a**[c]	52
5	**1b**	**2b**	10	10	**4b**[c]	55
6	**1c**	**2b**	10	10	**4c**[c]	67

[a] The coupling reactions were performed in diisopropylamine (20 mL) under nitrogen atmosphere for 18 h.
[b] Reactions were carried out at 65 °C.
[c] Reactions were carried out at 82 °C.

display peaks in the desired positions of the ^{13}C NMR spectra. It is to be noted that compound **3c** and **4a** were reported in earlier [25].

3.3. Thermal stability

Electronic device fabrication and their performance (life time and durability) depend on the thermal stability of materials [26a,19b]. Thermal stability of **3a-c** and **4a-c** (Fig. 3) were evaluated by thermo gravimetric analysis (TGA) and differential scanning calorimetry (DSC) under nitrogen atmosphere. Nitrophenyl substituted alkoxyphenylene ethynylenes **3a-c** displays good thermal stability (Table 3), and their stabilities do not significantly depend on the alkoxy side chain (T_5 329 °C for **3a**, T_5 326 °C for **3b**, T_5 321 °C for **3c**).

In contrast, the thermal stability of tolyl substituted alkoxyphenylene ethynylenes **4a-c** increases when alkoxy chain length increases (Fig. 3) from OC_4H_9 (T_5 288 °C for **4a**) to OC_8H_{17} (T_5 338 °C for **4b**) to $C_{12}H_{25}$ (T_5 347 °C for **4c**). It is also observed that thermal stability of **4a-c** is higher than that of **3a-c**.

Analysis of the TG traces (heating rate 10 °C/min) shows that the decomposition of the compound follows successive order. In **3a** and **3c**, loss of NO_2 is detected in the first step (Wt. loss: **3a** Calc. 17%, Found 17%; **3b** Calc. 15%, Found 18%). In **4a**, loss of tolyl group is observed in first step (Wt. loss, Calc. 40%, Found 42%), and loss of C_2H_5 group is observed in second step (Wt. loss, Calc. 12%, Found 11%). In compound **4b**, loss of C_4H_9 (Wt. loss, Calc. 20%, Found 21%) and OC_4H_9 (Wt. loss, Calc. 25%, Found 28%) is observed consecutively. Representative TGA curve of compound **3a** is given in Supplementary information.

In DSC thermograms, compounds **3a-c** display crystal to liquid transitions on heating, and liquid to crystal transition on cooling cycle. Transition temperatures of **3a-c** and **4a-c** are summarized in Table 4. It is observed that melting temperature decreases with increasing alkoxy chain length. However, in **4a-c**, melting temperature decreases from **4a** to **4b**, but it shows slight increase from **4b** to **4c** (Table 4).

In contrast to **4a-4b**, DSC traces of **4c** displays three endothermic transitions at 63, 65 and 69 °C during first heating, but on second heating only one transition is observed. On first cooling, it shows a shoulder before exothermic transition. However, on second cooling, it displays only one transition. These endothermic transitions during first heating may be due to the irreversible crystal to crystal transitions. Similar structural transitions are not rare in inorganic and organic compounds [26b-c].

3.4. Optical absorption and emission properties

Compounds **3a-c** displays two bands at 339 and 410 nm in the UV–Vis spectra (Fig. 4). The phenylethylnyl π system of the compounds is modified by the oxygen lone pair of alkoxy side chain leading to the formation of two HOMO systems: HOMO-1 and HOMO-2, and transitions from these orbitals to the LUMO results two separate bands (Table 5) [27]. These absorption bands are unaffected with the variation of alkoxy chain from OC_4H_9 to OC_8H_{17} then $OC_{12}H_{25}$. However, if the electron withdrawing nitro phenyl group is replaced by electron donating tolyl group as in **4a-c**, the absorption band is blue shifted to 309 and 368 nm. This observation suggests that in **3a-c,** electron withdrawing NO_2 groups delocalizes Π-electron on the whole molecule to stabilize quinoid structure [1a] thus lowering the absorption energy [19c].

The room temperature photoluminescence spectra, in dichloromethane, for compounds **3a-c** and **4a-c** were recorded under excitation at 410 and 370 nm, respectively (Table 5). The spectra are shown in Fig. 5 and Fig. 6. Compounds with electron withdrawing NO_2, **3a-b** displays emission band peaking at 555 nm, whereas that with electron donating CH_3 **4a-c** exhibit peaks at 403 nm (Table 5).

'Acceptor-donor-acceptor' (A-D-A) type trimers **3a-c** emit at a wide region of wavelengths: blue-green whereas 'donor-donor-donor' (D-D-D) type trimers **4a-c** show emission in the blue region. This observation is consistent with previous reports of conjugated ethynyl oligomers [19]. Stokes' shift of **3a-b** is 145 nm which is larger than that for **4a-c** (35 nm). It has been reported in the literature that ethynyl oligomers with donor-acceptor end groups give larger Stokes shift [19c]. However, in this study, ethynyl bridged trimers with acceptor-donor-acceptor type aromatic compounds **3a-c** gives larger shift than their congeners with donor-donor–donor type aromatic compounds **4a-c**. The large stokes shift may be associated with the emission from the intramolecular charge transfer states (delocalized LUMO levels) of the A-D-A type materials [19d–e]. Compounds with small shift are prone to

Table 2
Selected spectroscopic data for compounds **3a-b** and **4b-c.**

Compounds	IR (ν C≡C, cm^{-1})	^1H NMR (ppm)[a]	^{13}C NMR (ppm)
3a	2205	4.05 (t, ^3J = 6.4 Hz, 4H, OCH_2), 7.03 {s, 2H, $(RO)_2$Ar-*H*), 7.65 (d, ^3J = 8.80 Hz, 4H, C≡C-Ar-*H*), 8.22 (d, ^3J = 8.80 Hz, 4H, C≡C-Ar-*H*)	69.34 (OCH_2), 91.21 and 93.38 (*C*≡*C*)
3b	2205	4.04 (t, ^3J = 6.0 Hz, 4H, OCH_2), 7.02 {s, 2H, $(RO)_2$Ar-*H*), 7.65 (d, ^3J = 8.00 Hz, 4H, C≡C-Ar-*H*), 8.22 (d, ^3J = 7.60 Hz, 4H, C≡C-Ar-*H*)	69.62 (OCH_2), 91.22 and 93.38 (*C*≡*C*)
4b	2206	2.35 (s, 6H, Ar-CH_3), 4.01 (t, ^3J = 6.4 Hz, 4H, OCH_2), 6.98 {s, 2H, $(RO)_2$Ar-*H*}, 7.14 (d, ^3J = 7.60 Hz, 4H, C≡C-Ar-*H*), 7.42 (d, ^3J = 7.60 Hz, 4H, C≡C-Ar-*H*)	69.72 (OCH_2), 85.35 and 95.00 (*C*≡*C*)
4c	2212	2.36 (s, 6H, Ar-CH_3), 4.01 (t, ^3J = 6.0 Hz, 4H, OCH_2), 6.99 {s, 2H, $(RO)_2$Ar-*H*}, 7.14 (d, 4H, ^3J = 7.60 Hz, C≡C-Ar-*H*), 7.42 (d, 4H, ^3J = 7.20 Hz, C≡C-Ar-*H*)	69.71 (OCH_2), 85.37 and 95.00 (*C*≡*C*)

[a] ^1H NMR spectra were referenced to residual solvent ($CDCl_3$) resonances.

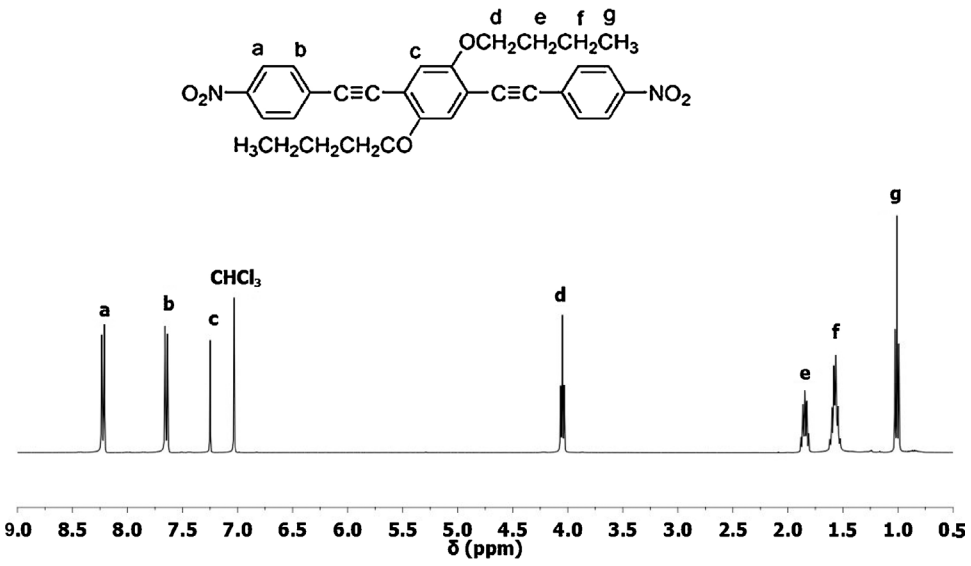

Fig. 2. ^{1}H NMR spectrum of compound **3a.**

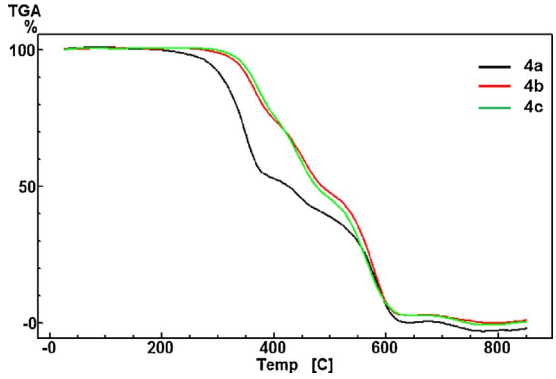

Fig. 3. TGA traces of compound **4a-c.**

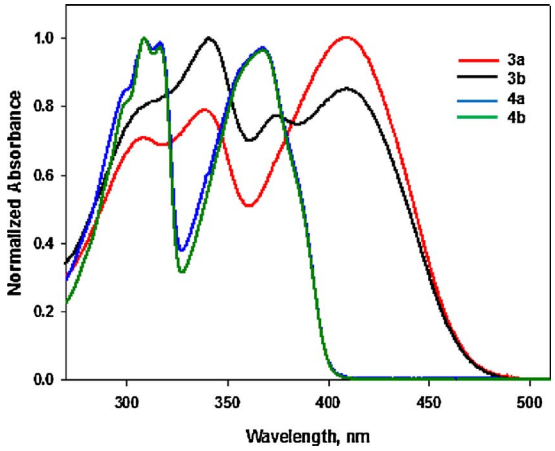

Fig. 4. UV–Vis absorption spectra of compounds **3a-b** and **4a-b** in $CHCl_3$, at room temperature.

Table 3
TGA data for compounds **3a-c** and **4a-c.**

Compounds	Decomposition Temperature (T_d)[a] (°C)	Decomposition Temperature (T_5)[b] (°C)
3a	199	329
3b	280	326
3c	252	321
4a	205	288
4b	281	338
4c	302	347

[a] Initial decomposition temperature (T_d).
[b] Temperature at which 5% weight is lost (T_5).

Table 4
Transition temperatures of **3a-c** and **4a-c** during second heating and cooling.

Compounds	Heating cycle[a]	Cooling cycle[a]
3a	Cr-L 211 °C	L-Cr 189 °C
3b	Cr-L 134 °C	L-Cr 117 °C
3c	Cr-L 131 °C	L-Cr 111 °C
4a	Cr-L 147 °C	L-Cr 138 °C
4b	Cr-L 58 °C	L-Cr [b]
4c	Cr-L 69 °C	L-Cr 43 °C

[a] Cr = Crystalline phase, L = Liquid phase.
[b] Not observed down to 25 °C.

Table 5
Absorption and photoluminescence data of compounds **3a-c** and **4a-c.**

Compounds	Absorption peaks, λ_{max} (nm)	Extinction Coefficient, ε[a] ($M^{-1}cm^{-1}$)	Emission peaks, λ[b] (nm)
3a	339, 410	46,659	555
3b	339, 410	51,607	555
3c	339, 410	47,010	407
4a	309, 368	9459	403
4b	309, 368	10,807	403
4c	309, 368	40,564	403

[a] Extinction coefficient is calculated for the lowest energy band.
[b] Sample concentrations are 1×10^5 M in chloroform at room temperature.

self-quenching, so large stokes shift is a useful feature for new materials which could be used as laser dyes and molecular imaging [19e].

3.5. Third-order nonlinear optical property

The most commonly used method for measuring the optical nonlinearity is the Z-scan method of Bahae [28a]. The method involves the transmission of a focused Gaussian beam of laser light through a sample. A convex lens is used for focusing the beam. The sample is translated along the z-axis. The transmitted light intensity is measured

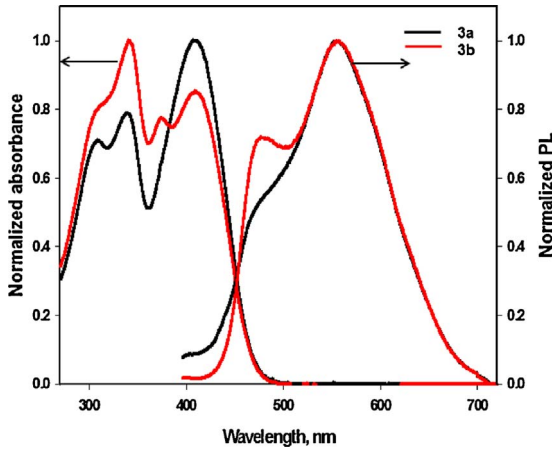

Fig. 5. Optical absorption and photoluminescence spectra of compounds **3a-c** in $CHCl_3$ at room temperature under excitation at 410 nm.

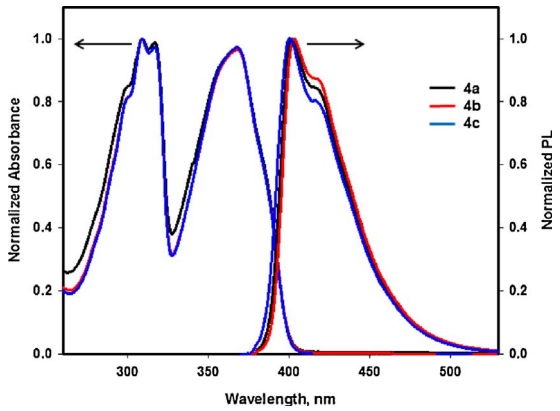

Fig. 6. Optical absorption and photoluminescence spectra of compounds **4a-c** in $CHCl_3$ at room temperature under excitation at 370 nm.

in the far field as the sample translation takes place within the focal point of the convex lens (Fig. 1). The refractive index of the sample changes according to [28]

$$n = n_0 + n_2 I$$

where n_0 is the linear refractive index, n_2 is the nonlinear refractive index and I is the intensity of incident light. When n_2 is positive, it gives rise to a positive lensing effect in the sample. n_2 is related to the nonlinear phase shift $\Delta\phi$ by

$$\Delta\phi = n_2 k I L_{eff}$$

where $L_{eff} = \frac{1-e^{-\alpha L}}{\alpha}$, L being the width of the sample and α be the linear absorption co-efficient.

A transmittance vs position plot obtained from the experimental data gives a peak-valley or valley-peak curve which is a signature of third-order nonlinearity: a peak-valley curve gives negative n_2 value and valley-peak gives positive n_2 value [28a]. Fig. 7 shows the closed aperture Z-scan traces for compound **3a-c**. The curves show a poor fit with the theoretical model in the positive z positions mainly due to the nonlocal effect produced by the incident laser beam [28b]. The thermal lens that is formed due to the incident laser is retained for relatively longer times so the fractional intensity change becomes slower. The transmittance traces of **3a-c** and **4a-c** show a prefocal peak followed by a post-focal valley which imply that the nonlinear refractive index are negative ($n_2 < 0$) suggesting self defocusing [29a]. The calculated peak-valley difference ΔT_{p-v} is found to be ~ 1.8 times the Rayleigh range Z_R reveals the nonlinearity is thermal in nature [29b]. Light

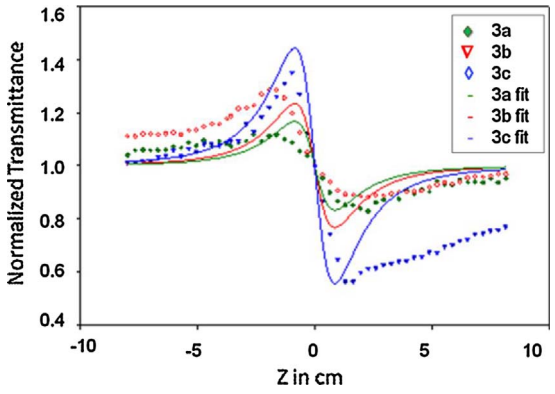

Fig. 7. Closed aperture Z-scan traces of **3a-c.**

absorption by the materials creates heat, and focusing and defocusing effect is observed due to the variation of refractive index with temperature where the material itself act as a thermal lens [29c–d].

In the A-D-A series **3a-c**, the n_2 values increase with increasing alkoxy chain length suggesting the interaction of alkoxy chains with intense laser light. In contrast, the variation of alkoxy chain shows no effect in the UV–Vis light (Fig. 4). The D-D–D series **4a-c** follows the same trend except that **4b** with OC_8H_{17} gives abnormally high value at lower concentration. The third-order NLO properties of poly(3-alkoxythiophene) also show a strong dependence on the alkoxy side chains [29e].

The NLO response increases with increase of concentration (Fig. 8) attributed to the increasing number of thermally agitated molecules that enhances the nonlinear refractive index value. A similar measurement technique on a phenothiazine system [29a] yields an n_2 value of the order of 10^{-7} cm^2/W. This is comparable to the value reported in this work (Table 6). However, literature shows that NLO properties of pi conjugated systems have also been investigated by femto second (pulse) lasers, γ values and nonlinear susceptibility $\chi^{(3)}$ were calculated [20e,29f] which are of the order of 10^{-23} cm^2/W. The resonance effects and other local effects come into play when ultra fast (femto second) nonlinearity is in consideration.

4. Conclusions

A series of acceptor and donor substituted bis(alkoxy)phenyleneethynylenes has been prepared and characterized. Thermal studies by thermogravimetric analysis (TGA) and differential scanning calorimetry (DSC) under nitrogen atmosphere demonstrate good thermal stability of the compounds. Acceptor substituted **3a-c** absorb longer wavelength in the UV–Vis spectra than that of donor substituted **4a-c**. In the emission spectra, **3a-c** emit in the green whereas **4a-c** emit in the blue region of

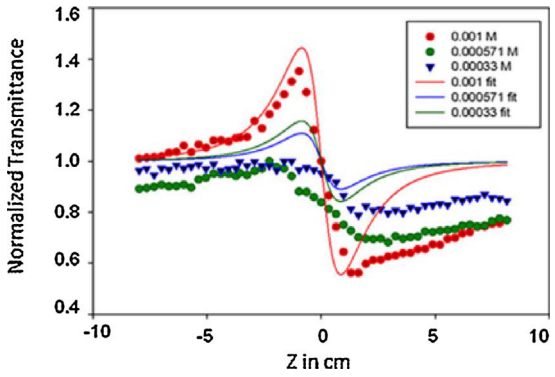

Fig. 8. Closed aperture Z scan trace of **3c** at different concentrations.

Table 6
Nonlinear refractive index (n_2) values of **3a-c** and **4a-c.**

Material	$\Delta\varphi \times 10^{-4}$	$n_2 \times 10^{-8}$ (cm^2/W)
3a	25	−0.97 ± 0.08
3b	23	−1.15 ± 0.10
3c	47	−2.34 ± 0.26
4a	11	−0.66 ± 0.08
4b	31	−1.67 ± 0.33
4c	16	−0.88 ± 0.08

Δφ: nonlinear phase shift of the incident beam.
Measurements were carried out at 1×10^{-3} M concentration.

the electromagnetic radiation. The closed aperture Z-scan technique suggests that the materials have third-order nonlinearity which varies with the acceptor and donor substitutents as well as alkoxy chain length.

Acknowledgements

We are grateful to the Higher Education Quality Enhancement Project (CP 2524) of the University Grants Commission of Bangladesh for funding.

Appendix A. Supplementary data

Supplementary data associated with this article can be found, in the online version, at http://dx.doi.org/10.1016/j.synthmet.2017.06.005.

The IR and NMR (^{1}H and 13C) spectra of all new compounds, and selected TGA and DSC thermograms are available.

References

[1] (a) L. Dou, Y. Liu, Z. Hong, G. Li, Y. Yang, Chem. Rev 115 (2015) 12633;
(b) P.-L.T. Boudreault, A. Najari, M. Leclerc, Chem. Mater. 23 (2011) 456.
[2] (a) L. Lu, T. Zheng, Q. Wu, A.M. Schneider, D. Zhao, L. Yu, Chem. Rev. 115 (2015) 12666;
(b) Y.-J. Cheng, S.-H. Yang, C.-S. Hsu, Chem. Rev. 109 (2009) 5868.
[3] B. Carsten, F. He, H.J. Son, T. Xu, L. Yu, Chem. Rev. 111 (2011) 1493.
[4] X. Guo, A. Facchetti, T.J. Marks, Chem. Rev. 114 (2014) 8943.
[5] A.C. Grimsdale, K.L. Chan, R.E. Martin, P.G. Jokisz, A.B. Holmes, Chem. Rev. 109 (2009) 897.
[6] H. Sirringhaus, Nat. Mater. 2 (2003) 641.
[7] (a) A. Pron, P.P. Rannou, Polym. Sci. 27 (2002) 135;
(b) F. Cacialli, F. Phil, Trans. R. Soc Lond. A 358 (2000) 173.
[8] (a) W. Kowalsky, E. Becker, T. Benstem, H.-H. Johannes, D. Metzdorf, H. Neuner, J. Schobel, Solid State Phys. 40 (2000) 795;
(b) G. Horowitz, Adv. Mater 2 (1990) 287.
[9] R.W. Boyd, Nonlinear Optics, third edition, Elsevier Ltd, Oxford, 2008.
[10] (a) U.H.F. Bunz, Chem. Rev. 100 (2000) 1605;
(b) U.H.F. Bunz, Macromol, Rapid Commun. 30 (2009) 772.
[11] (a) H.A. Dieck, R.F. Heck, J. Organomet Chem. 93 (1975) 259;
(b) L. Cassar, J. Organomet. Chem. 93 (1975) 253.
[12] K. Sonogashira, Y. Tohda, N. Hagihara, Tetrahedron Lett. (1975) 4467.
[13] K. Sanechika, T. Yamamoto, A. Yamamoto, Bull. Chem. Soc. Jpn 57 (1984) 752.
[14] S.R. Havens, P.M. Hergenrother, J. Polym. Sci. Polym. Lett. 23 (1985) 587.
[15] D.L. Trumbo, C.S. Marvel, J. Polym, Sci. Polym. Chem. Ed. 24 (1986) 2311.
[16] (a) R. Giesa, R.C. Schulz, Makmmol Chem. 191 (1990) 857;
(b) M. Moroni, J.L. Moigne, Macromolecules 27 (1994) 562;
(c) V. Francke, T. Mangel, K. Mullen, Macromolecules 31 (1998) 2447.
[17] G. Voskerician, C. Weder, Adv. Polym. Sci. 177 (2005) 209.
[18] Y. Lin, Y. Li, X. Zhan, Chem. Soc. Rev. 41 (2012) 4245.
[19] (a) X. Bai, X. Chen, J.R. Dias, T.C. Sandreczki, Tetrahedron Lett. 54 (2013) 1711;
(b) V. Ervithayasuporn, J. Abe, X. Wang, T. Matsushima, H. Murata, Y. Kawakami, Tetrahedron 66 (2010) 9348;
(c) Z. Zhao, X. Xu, F. Wang, G. Yu, P. Lu, Y. Liu, D. Zhu, Synthetic Metals 156 (2006) 209;
(d) P. Horvath, P. Sebej, T. Solomek, P. Klan, J. Org. Chem. 80 (2015) 1299;
(e) T. Dutta, K.B. Woody, S.R. Parkin, M.D. Watson, J. Gierschner, J. Am. Chem. Soc. 131 (2009) 17321.
[20] W. Liang, Z. Gao, W. Song, J. Su, K. Guo, Q. Dong, J. Huang, W.-Y. Wong, Tetrahedron 72 (2016) 1505.
[21] (a) K. Koynov, A. Bahtiar, C. Bubeck, B. Muhling, H. Meier, J. Phy. Chem. B 109 (2005) 10184;
(b) K. Koishi, T. Ikeda, K. Kondo, T. Sakaguchi, K. Kamada, K. Tawa, K. Ohta, Macromol. Chem Plys 201 (2000) 525;
(c) M.S. Wong, Z.H. Li, M.F. Shek, M. Samoc, A. Samoc, B. Luther-Davies, Chem. Mater. 14 (2002) 2999;
(d) D.A.M. Egbe, R. Stockmann, M. Hotzel, J. Opt A.: Pure. Appl. Opt. 6 (2004) 791;
(e) H.E. Quazzani, K. Iliopoulos, M. Pranaitis, O. Krupka, V. Smokal, A. Kolendo, B. Sahraoui, J. Phys, Chem. B 115 (2010) 1944;
(f) B. Sahraoui, G. Rivoire, N. Terkia-Derdra, M. Salle, J. Zaremba, J. Opt. Soc. Am. B 15 (1998) 923.
[22] W.L.F. Armarego, D.D. Perrin, Purification of Laboratory Chemicals, 4th ed., Butterworth-Heinemann, Guildford UK, 1996.
[23] Z. Bao, Y. Chen, R. Cai, L. Yu, Macromolecules 26 (1993) 5281.
[24] S. Takahashi, Y. Kuroyama, K. Sonogahara, N. Hagihara, Synthesis 8 (1980) 627.
[25] (a) X.-Y. Chen, C. Barnes, J.R. Dias, T.C. Sandreczki, Chem. Eur. J. 15 (2009) 2041;
(b) A. Harriman, L.J. Mallon, K.J. Elliot, A. Haefele, G. Ulrich, R. Ziessel, J. Am. Chem. Soc. 131 (2009) 13375.
[26] (a) Y. Qian, F. Cao, W. Guo, Tetrahedron 69 (2013) 4169;
(b) K. Suzuki, F. Nakamura, Y. Eonomoto, T. Asaza, T. Hashimoto, H. Ohki, S. Ishimaru, R. Ikeda, F. Shimuzu, M. Takashige, O. Yamamuro, S. Hayashi, Thermochemica Acta 431 (2005) 73;
(c) H.O. Desseyn, K. Clou, J.F. Janssens, R. Carleer, Therochemica Acta 402 (2003) 81.
[27] (a) P.V. James, P.K. Sudeep, C.H. Suresh, K.G. Thomas, J. Phys. Chem. A 110 (2006) 4329;
(b) O.K. Nag, K.M. Anis-Ul-Haque, D. Debnath, R. Begum, M. Younus, N. Chawdhury, G. Kociok-Köhn, P.R. Raithby, J. Chem. Sci. 127 (2015) 365.
[28] (a) M. Sheikh-Bahae, A.A. Said, T.H. Wei, D.J. Hagan, E.W.V. Strylan, J. IEEE Quantum Electronics 26 (1990) 760;
(b) F.L.S. Cuppo, A.M.F. Neto, S.L. Gómez, P. Palffy-Muhoray, JOSA B 19 (2002) 1342.
[29] (a) R.M. El-Shishtawy, F.A.M. Al-Zahrani, S.M. Afzal, M.A.N. Razvi, Z.M. Al-Mashany, A.H. Bakry, A.M. Ashiri, RSC Adv. 6 (2016) 91546;
(b) R. Ponnusamy, D. Sivasubramanian, P. Sreekanth, V. Gandhiraj, R. Philip, G.M. Bhalerao, RSC Adv. 5 (2015) 80756;
(c) H.A. Badran, Appl. Phys. B 119 (2015) 319;
(d) M.K. Biswas, M.K. Amin, P.K. Das, E. Hoque, S.M. Sharafuddin, M. Younus, S.K. Das, Y. Haque, J. Non. Opt. Phys Mat 24 (2015) 1550039;
(e) D. Yanmao, J. Lu, Q. Xu, F. Yan, X. Xia, L. Wang, L. Hu, Synth. Met. 160 (2010) 409;
(f) K. Iliopoulos, A. El-Ghayoury, H. El-Ouazzani, M. Pranaitis, E. Belhadj, E. Ripaud, M. Mazari, M. Sallé, D. Gindre, B. Sahraoui, Optics express 20 (2012) 25311.